HHS Public Access

Author manuscript

Endocr Relat Cancer. Author manuscript; available in PMC 2020 September 07.

Published in final edited form as:

Endocr Relat Cancer. 2019 August ; 26(8): 727–738. doi:10.1530/ERC-18-0555.

Targeting PLKs as a Therapeutic Approach to Well-differentiated Thyroid Cancer

Shu-Fu Lin[1,2,*], **Jen-Der Lin**[1,2], **Chun-Nan Yeh**[2,3], **Yu-Tung Huang**[4], **Ting-Chao Chou**[5,6], **Richard J. Wong**[7]

[1]Department of Internal Medicine, Chang Gung Memorial Hospital, Taoyuan, Taiwan

[2]Chang Gung University, Taoyuan, Taiwan

[3]Department of Surgery, Chang Gung Memorial Hospital, Taoyuan, Taiwan

[4]Center for Big Data Analytics and Statistics, Chang Gung Memorial Hospital, Taoyuan, Taiwan

[5]Laboratory of Preclinical Pharmacology Core, Memorial Sloan-Kettering Cancer Center, New York, NY, USA

[6]Current address: PD Science, Inc., 599 Mill Run, Paramus, NJ, USA

[7]Department of Surgery, Memorial Sloan-Kettering Cancer Center, New York, NY, USA

Abstract

Polo-like kinases (PLKs) are pivotal regulators of cell proliferation and cell survival; therefore, PLKs may be potential targets in the treatment of malignancy. The therapeutic effects of volasertib, a PLKs inhibitor for papillary and follicular thyroid cancer (known as well-differentiated thyroid cancer) were evaluated in this study. Volasertib inhibited cell proliferation in two papillary and two follicular thyroid cancer cell lines in a dose-dependent manner. Volasertib treatment reduced cells in S phase and increased cells in G2/M phase. Volasertib activated caspase-3 activity and induced apoptosis. Drug combinations of volasertib and sorafenib showed mostly synergism in four well-differentiated thyroid carcinoma cell lines *in vitro*. Volasertib treatment *in vivo* retarded the growth of a papillary thyroid tumor model. Furthermore, the combination of volasertib with sorafenib was more effective than either single treatment in a follicular thyroid cancer xenograft model. Promising safety profiles appeared in animals treated with either volasertib alone or volasertib and sorafenib combination therapy. These findings support volasertib as a potential drug for the treatment of patients with well-differentiated thyroid cancer.

[*]**Corresponding author:** Shu-Fu Lin, Department of Internal Medicine, Chang Gung Memorial Hospital, Taoyuan, Taiwan; mmg@cgmh.org.tw; Tel: +886 3 3281200 ext 8821; Fax: +886 3 3288257.

Author contributions

S-F L and C-N Y conceived the work; S-F L and R W designed the study; J-D L, T-C C and R W provided material support; S-F L acquired the data; all authors analyzed and interpreted the data; S-F L wrote the manuscript; and all authors reviewed and revised the manuscript.

Declaration of interest

There is no potential conflict of interest.

Keywords

volasertib; polo-like kinase inhibitor; sorafenib; well-differentiated thyroid cancer

Introduction

The incidence of thyroid cancer has increased worldwide over the past four decades (Kitahara & Sosa 2016, Cabanillas *et al.* 2016). The transformation of thyroid follicular cells leads to different types of thyroid malignancy, including papillary and follicular thyroid cancer (known as well-differentiated thyroid cancer), poorly-differentiated and anaplastic thyroid cancer (Fagin & Wells 2016). Well-differentiated thyroid cancer (WDTC) accounts for more than 85% of patients with thyroid carcinoma. Most patients with WDTC survive for more than 10 years after diagnosis following standard treatment with surgery, radioactive iodine (RAI) and thyroid hormone therapy. However, a small proportion of patients who develop metastatic RAI-refractory WDTC have the mean life expectancy of 3–5 years and the 10-year survival rate is only 10% (Durante *et al.* 2006). Two multi-kinase inhibitors, sorafenib and lenvatinib, have been approved for the treatment of metastatic and RAI-refractory WDTC by the U.S. Food and Drug Administration (FDA). However, many patients acquire resistance to these drugs or experience toxicities, resulting in dose reduction and termination of treatment (Brose *et al.* 2014, Schlumberger *et al.* 2015). Novel therapeutic strategies with distinct mechanisms are mandatory to meet the clinical needs of patients with aggressive WDTC.

Polo-like kinases (PLKs) are a family of serine/threonine kinases that performs multiple cellular functions, including cell cycle progression and cell survival (Zitouni *et al.* 2014, Strebhardt *et al.* 2010). There are five human PLK family proteins (PLK1–5) (de Cárcer *et al.* 2011*a*). PLK1 regulates centrosome maturation, mitotic progression, DNA damage repair and inhibition of apoptosis (Zitouni *et al.* 2014, Yata *et al.* 2012, Shao *et al.* 2018, Liu & Erikson 2003). PLK2 and PLK4 are required for centrosome duplication (Cizmecioglu *et al.* 2012, Habedanck *et al.* 2005). PLK3 is involved in DNA replication, G1/S and G2/M transition, and induction of apoptosis under stress conditions (Zitouni *et al.* 2014, Helmke *et al.* 2016). PLK5 is mostly expressed in the brain and may function as a tumor suppressor (de Cárcer *et al.* 2011*b*). Given the essential roles of PLKs function in cell proliferation and cell survival, PLKs are attractive targets for anticancer therapy and a variety of PLK inhibitors have been evaluated in the treatment of malignancies (Sebastian *et al.* 2010, Zitouni *et al.* 2014, Gjertsen *et al.* 2015, Kosco *et al.* 2018).

Volasertib is a potent inhibitor of PLK1, PLK2 and PLK3, with 50% inhibitory concentrations in nanomolar range (0.87 nmol/L, 5 nmol/L, and 56 nmol/L, respectively) (Rudolph *et al.* 2009). Volasertib has been shown to induce G2/M arrest, activate caspase-3 activity and induce apoptosis *in vitro* (Nguyen *et al.* 2017). Administration of volasertib has good tissue penetration, a long terminal half-life and potent efficacy in inhibiting tumor growth of colon, lymphoma and leukemia xenografts, with promising safety profiles in animal models (Nguyen *et al.* 2017, Rudolph *et al.* 2009, Rudolph *et al.* 2015). Recently, single-agent volasertib therapy has revealed encouraging antitumor activity in patients with

ovarian cancer in a phase II clinical trial (Pujade-Lauraine *et al*. 2016). In this study, we sought to evaluate the therapeutic effects of volasertib alone and in combination with sorafenib, a multi-kinase inhibitor approved for the treatment of thyroid cancer, in WDTC *in vitro* and *in vivo*.

Materials and Methods

Cell lines

Two human papillary thyroid cancer cell lines, BHP7–13 and K1, and two human follicular thyroid cancer cell lines, FTC-133 and RO82-W-1, were studied. BHP7–13 cells were described before (Lin *et al*. 2017). K1, FTC-133 and RO82-W-1were obtained from Sigma. All cell lines except RO82-W-1 were authenticated using DNA short tandem repeats (STR) profiling and stored in liquid nitrogen until use (Schweppe *et al*. 2008). BHP7–13 and TPC1 are considered genetically identical cell lines because they have identical DNA STR profiling (Schweppe *et al*. 2008). BHP7–13 cells were maintained in RPMI 1640 with sodium bicarbonate (2.0 g/L). K1 and RO82-W-1 cells were maintained in DMEM, Ham's F12 and MCDB 105 (2:1:1) with glutamine (2.0 mmol/L). FTC-133 cells were maintained in DMEM and Ham's F12 (1:1) with glutamine (2.0 mmol/L). All media contained 10% fetal calf serum, 100,000 units/L penicillin and 100 mg/L streptomycin. All cells were maintained in a 5% CO_2 humidified incubator at 37°C. The maximum passage number of WDTC cells after thawing was limited to 20 for this study.

Pharmacologic agents

Volasertib, sorafenib and GSK461364 were obtained from Selleck Chemicals. Volasertib, sorafenib and GSK461364 were dissolved in DMSO (Sigma) to a concentration of 10 mmol/L and stored at −80°C until further use for *in vitro* experiments. For the *in vivo* studies, volasertib was diluted in poly(ethylene glycol) 300 (Sigma) and distilled water (2:3 v/v) to a final concentration of 3 mg/ml and stored at −80 ºC until use. Sorafenib was dissolved in 50% Kolliphor EL (Sigma) and 50% ethanol (Sigma) to a concentration of 57.6 mg/mL and stored at −80°C. Sorafenib was further diluted with water to a final concentration of 14.4 mg/mL before *in vivo* use.

Antibodies

Antibodies targeting cleaved caspase-3, proliferating cell nuclear antigen (PCNA), p-Histone H3 (Ser10), PLK1, PLK2 and PLK3 were purchased from Cell Signaling Technology. α-tubulin and β-actin antibodies were obtained from Sigma.

Cytotoxicity assays and drug synergy studies

Cells were plated at 2×10^3 (BHP7–13 and FTC-133) and 2×10^4 cells (K1 and RO82-W-1) per well in 24-well plates in 1 mL of media. After overnight incubation, six serial two-fold dilutions of volasertib, sorafenib or vehicle were added over a 4-day treatment course after which cytotoxicity was determined. Culture medium was removed, and the cells were washed with PBS and lysed with Triton X-100 (1.35%, Sigma) to release intracellular lactate dehydrogenase (LDH), which was quantified with a Cytotox 96 kit (Promega) at 490 nm by spectrophotometry (Infinite M200 PRO, Tecan). Each experiment was performed in

triplicate, and the results are shown as the percentage of surviving cells determined by comparing the LDH of each sample relative to control samples, which were considered 100% viable. The median-effect dose (IC_{50}) on day 4 was calculated for each cell line using CompuSyn software (Chou & Martin 2005, Chou 2006).

For combination therapy studies, cells were treated with volasertib and sorafenib at a fixed dose ratio. Cells were incubated with vehicle, volasertib, sorafenib or combination therapy simultaneously for a 4-day course after which cytotoxicity was measured. Interactions between volasertib and sorafenib *in vitro* were assessed by calculating the combination index (CI) using the Chou-Talalay equation and CompuSyn software. Synergy (CI < 1), additive effect (CI = 1) and antagonism (CI > 1) are quantitatively determined by CompuSyn simulation at different effect levels.

Cell cycle assessment

The effects of volasertib on cell cycle progression were evaluated. Cells were plated at 4×10^5 cells per well in 6-well plates in 2 mL of media overnight. Volasertib (100 nmol/L) or vehicle was added and incubated for 24 h, after which adherent cells were collected, washed with PBS, fixed with cold 70% ethanol and incubated with RNase A (100 μg/mL; Sigma) and propidium iodide (5 μg/mL; Sigma) at 37°C for 15 min. Cell cycle distribution was assessed by DNA content detected by flow cytometry (BD FACScalibur Flow Cytometer, BD Biosciences). Each condition was performed in triplicate.

Apoptosis assessment

Caspase-3 activity was analyzed using a fluorometric assay kit (Abcam). Cells were plated at 1×10^6 cells in 100-mm Petri dishes in 10 mL of media overnight. Volasertib (100 nmol/L) or vehicle was added for 24 h. Adherent cells (5×10^5) were collected, centrifuged and lysed using 50 μL of lysis buffer on ice for 10 min, and incubated with DEVD-AFC substrate and reaction buffer at 37°C for 1.5 h. Caspase-3 activity was detected by spectrophotometry. Each condition was performed in duplicate.

The ability of volasertib to induce sub-G1 apoptotic cell accumulation was studied using flow cytometry. Cells were plated at 2×10^5 (BHP7–13) or 4×10^5 (K1, FTC-133, RO82-W-1) cells per well in 6-well plates in 2 mL media overnight. Volasertib (100 nmol/L) or vehicle was added and incubated for 24 h. Floating cells and trypsinized adherent cells were collected, and samples were prepared as described above for cell cycle assessment. Apoptotic sub-G1 cells were assessed by DNA content detected by flow cytometry (BD FACScalibur Flow Cytometer, BD Biosciences). Each condition was performed in triplicate.

Immunofluorescence microscopy

The expression of cleaved caspase-3 was evaluated using immunofluorescence microscopy. Thyroid cancer cells were plated at 5×10^4 cells in 4-well culture slides in 1 mL of media overnight. Cells were treated with volasertib (100 nmol/L) or placebo for 24 h, washed with PBS, fixed in 4% paraformaldehyde (Sigma) for 15 min at room temperature, washed with PBS, permeabilized with 0.1% Triton X-100 (10 min, room temperature) and washed with PBS. Cells were then incubated with primary rabbit cleaved caspase-3 antibody (1:400) and

mouse α-tubulin antibody (1:1000) at 4°C overnight, washed with PBS and incubated with secondary Alexa Fluor 633-conjugated goat anti-rabbit antibody (1:1000; Invitrogen) and Alexa Fluor 488-conjugated goat anti-mouse antibody (1:1000; Life Technologies) for 25 min at 37°C, washed with PBS, incubated with 4′,6-diamidino-2-phenylindole (DAPI; 0.2 μg/mL, Invitrogen) for 10 min at room temperature, washed with PBS and covered with mounting medium. Images were acquired using Leica TCS SP8 X confocal microscopy (Leica Microsystems).

The effect of volasertib on mitosis was evaluated using confocal microscopy. Thyroid cancer cells were plated at 1×10^5 cells in 4-well culture slides in 1 mL of media overnight. Volasertib (100 nmol/L) or placebo-treated thyroid cancer cell samples were prepared as described above. Cells were then incubated with primary rabbit p-Histone H3 (Ser10) (1:200) and mouse α-tubulin antibody (1:1000) at 4°C overnight, washed with PBS, incubated with secondary Alexa Fluor 633-conjugated goat anti-rabbit antibody (1:1000) and Alexa Fluor 488-conjugated goat anti-mouse antibody (1:1000) for 25 min at 37°C, then samples were prepared as described above. Images were captured with Leica TCS SP8 X confocal microscopy (Leica Microsystems). Chromosomes were examined to identify mitotic cells.

Flank xenograft tumor therapy

K1 and FTC-133 flank tumors were established by injecting 1×10^6 cells in 100 μL of extracellular matrix (ECM) gel (Sigma) into the subcutaneous flanks of female athymic nude mice 10–11 weeks of age from the National Laboratory Animal Center, Taiwan. K1 and FTC-133 cell lines were chosen because they had high tumorigenesis rates in murine models.

For monotherapy with volasertib, mice bearing K1 xenograft tumors received oral administration of vehicle or volasertib (25 mg/kg and 30 mg/kg) once a day for two cycles of 2-day on and 5-day off therapy. For volasertib and sorafenib combination oral therapy, mice bearing K1 and FTC-133 thyroid tumors received placebo, volasertib (25 mg/kg) once a day of 2-day on and 5-day off therapy, sorafenib (25 mg/kg) once a day of 4-day on and 3-day off therapy, or combination treatment for three cycles of therapy. Tumor dimensions were serially measured with electronic calipers, and the volumes were calculated by the following formula: $a \times b^2 \times 0.4$, where a represents the largest diameter and b is the perpendicular diameter. The body weight of each animal was followed as a marker of toxicity. Relative tumor growth of each xenograft was calculated as $Vx/V1$, where Vx is the volume in mm^3 at an indicated time and $V1$ at the beginning of treatment.

Tumor levels of PCNA (a marker for cell proliferation) (Moldovan *et al.* 2007) and cleaved caspase-3 were evaluated in mice treated with oral dosing of volasertib (25 mg/kg) by Western blot analysis. At indicated periods, animals were euthanized with carbon dioxide, and the tumors were harvested, mixed with protein extraction buffer (GE Healthcare), homogenized and sonicated on ice. After centrifugation, clarified supernatants were aliquoted and stored at −80°C until Western blot analyses.

This study was approved by the Committee of Laboratory Animal Center at the Chang Gung Memorial Hospital, Linkou (permission No: 2013121401) and performed in accordance with the recommendations in the Guide for the Care and Use of Laboratory Animals of the Chang Gung Memorial Hospital.

Western blot analysis

Thyroid tumor samples were collected and prepared as described above. Total protein (20–40 μg) was separated by electrophoresis on 12% Tris-HCl gels, transferred to polyvinylidene difluoride membranes, blocked and exposed to primary antibodies followed by a secondary antibody conjugated to horseradish peroxidase. Signals were developed using an enhanced chemiluminescence kit (PerkinElmer and Merck Millipore).

Statistical analyses

Statistical analyses were performed using IBM SPSS software (version 25). Kolmogorov-Smirnov test was used for assessment of normality. Student t test was carried out to analyze *in vitro* data. *In vivo* data were analyzed by two-way ANOVA with post-hoc Scheffe test. Pearson's correlation coefficient was used to measure the association between IC_{50} of volasertib and the expression of PLK1, PLK2 and PLK3 in four WDTC cell lines. Results are expressed as mean ± SE. $P < 0.05$ was considered statistically significant.

Results

Cytotoxicity of volasertib in WDTC cell lines

Volasertib inhibited cell survival in two papillary thyroid cancer cell lines (BHP7–13 and K1 cells) and two follicular thyroid cancer cell lines (FTC-133 and RO82-W-1 cells) in a dose-dependent manner (Fig. 1A). Volasertib at 100 nmol/L arrested cell growth by 99.1% (BHP7–13), 76.0% (K1), 77.5% (FTC-133) and 57.7% (RO82-W-1) on day 4. The cytotoxicity potency of volasertib in WDTC cell lines was determined using CompuSyn software. The median-effect dose (IC_{50}) was determined on day 4 (Fig. 1B). In papillary thyroid cancer cell lines, BHP7–13 cells had a lower IC_{50} (18.1 ± 0.0 nmol/L) than that of K1 cells (59.8 ± 0.6 nmol/L). In follicular thyroid cancer cell lines, FTC-133 cells had a lower IC_{50} (21.6 ± 0.8 nmol/L) than that of RO82-W-1 cells (71.5 ± 2.7 nmol/L).

Effects of volasertib on the cell cycle

The effect of volasertib (100 nmol/L for 24 h) on cell cycle distribution in papillary and follicular thyroid cancer cell lines was evaluated (Supplementary Fig. 1), and the cell cycle data was analyzed (Fig. 2A). Compared with placebo treatment, volasertib significantly induced cell accumulation in the G2/M phase as compared with control treatment in BHP7–13 (64.2 ± 0.5% and 8.5 ± 0.1%, $P < 0.001$), K1 (22.1 ± 0.2% and 10.2 ± 0.1%, $P < 0.001$), FTC-133 (82.1 ± 0.3% and 12.2 ± 0.1%, $P < 0.001$) and RO82-W-1 cells (85.5 ± 0.3% and 13.9 ± 0.1%, $P < 0.001$). Besides, volasertib significantly decreased cells in the S phase in BHP7–13 (3.8 ± 0.3% and 8.9 ± 0.2%, $P < 0.001$), K1 (10.5 ± 0.0% and 12.7 ± 0.2%, $P < 0.001$), FTC-133 (4.1 ± 0.1% and 5.6 ± 0.2%, $P = 0.002$) and RO82-W-1 cells (4.7 ± 0.2% and 8.1± 0.1%, $P < 0.001$).

The ability of volasertib to arrest cells in the mitotic phase was determined using confocal microscopy. A representative cell line, BHP7–13 cells, is shown (Supplementary Fig. 2). Mitotic cells were identified, and the mitotic index was calculated for papillary and follicular thyroid cancer cell lines (Fig. 2B). Compared with the control treatment, volasertib (100 nmol/L) treatment for 24 h significantly increased the percentage of mitotic cells in BHP7–13 (7.9 ± 1.5% and 2.4 ± 0.2%, P=0.002), K1 (3.6 ± 0.4% and 1.2 ± 0.2%, $P < 0.001$), FTC-133 (5.2 ± 0.5% and 2.6 ± 0.3%, $P < 0.001$) and RO82-W-1 cells (9.6 ± 0.9% and 1.6 ± 0.2%, $P < 0.001$), demonstrating that volasertib accumulated thyroid cancer cells in mitosis.

The distribution of cells in mitosis was evaluated (Fig. 2C). Compared with control treatment, volasertib (100 nmol/L for 24 h) significantly increased the percentage of prometaphase cells in BHP7–13, K1, FTC-133 and RO82-W-1. This finding of mitotic arrest in prometaphase is a characteristic phenotype of polo-like kinase arrest.

Volasertib induced apoptosis in WDTC cell lines

Induction of apoptosis has an important role in cancer therapy (Pfeffer & Singh 2018). Volasertib activates caspase-3 activity and induces apoptosis in lymphoma cells (Nguyen *et al.* 2017). Therefore, we evaluated the effects of volasertib on apoptosis in papillary and follicular thyroid cancer cell lines. The effects of volasertib (100 nmol/L) on caspase-3 activity in BHP7–13, K1, FTC-133 and RO82-W-1 cell lines were determined using a fluorometric assay at 24 h (Fig. 3A). Volasertib significantly increased caspase-3 activity compared to control treatment in BHP7–13, K1, FTC-133 and RO82-W-1 cells, demonstrating activation of caspase-3. Caspase-3 activation was also assessed by detection of cleaved caspase-3 using immunofluorescent analysis in papillary and follicular thyroid cancer cell lines (Fig. 3B). The percentages of cells with cleaved caspase-3 (active form of caspase-3) expression were analyzed (Fig. 3C). Volasertib (100 nmol/L for 24 h) significantly increased the proportions of cells with cleaved caspase-3 expression in BHP7–13, K1, FTC-133 and RO82-W-1 cells when compared with the corresponding controls. Therefore, activation of caspase-3 may lead to apoptotic cell death.

The ability of volasertib to induce sub-G1 apoptosis in papillary and follicular thyroid cancer cell lines was evaluated (Supplementary Fig. 3). BHP7–13, K1, FTC-133 and RO82-W-1 cell lines were exposed to volasertib (100 nmol/L for 24 h), and the proportion of sub-G1 apoptotic cells was calculated (Fig. 3D). Volasertib significantly induced higher proportions of sub-G1 cells in BHP7–13 (1.3 ± 0.0% and 0.5 ± 0.1%, $P = 0.001$), K1 (7.9 ± 0.2% and 5.1 ± 0.1%, $P < 0.001$), FTC-133 (9.1 ± 0.2% and 5.2 ± 0.2%, $P < 0.001$) and RO82-W-1 cells (1.7 ± 0.1% and 1.0 ± 0.0%, $P = 0.004$) as compared to the control treatment. These data indicate that volasertib induces apoptosis in papillary and follicular thyroid cancer cells.

Monotherapy with volasertib for murine flank WDTC tumors

Female nude mice bearing flank xenografts of K1 cells were used to evaluate the therapeutic efficacy and safety of volasertib in papillary thyroid cancer *in vivo*. Animals with established K1 flank tumors with a mean diameter of 4.8 mm were treated with oral gavage of placebo ($n = 6$), low-dose volasertib (25 mg/kg, $n = 6$) or high-dose volasertib (30 mg/kg, $n = 6$)

once a day for two cycles of a 2-day on and 5-day off therapy (Fig. 4A). Low-dose and high-dose volasertib treatment significantly retarded K1 tumor growth as compared to the control group ($P < 0.001$ and $P < 0.001$, respectively). Serial administration of low- and high-dose volasertib did not result in significant body weight change during the study period (Fig. 4B). We did not observe any morbidity in these animals. Representative mice bearing K1 tumors (Fig. 4C) were photographed after a 14-day treatment.

The molecular effects of low-dose volasertib (25 mg/kg) treatment in K1 xenografts were evaluated using Western blot analysis (Fig. 4D). Volasertib treatment increased the levels of cleaved caspase-3 on days 2 and 3. PCNA level was decreased by day 3.

Interaction of volasertib and sorafenib in WDTC cells

Interactions between volasertib and sorafenib were studied in papillary and follicular thyroid cancer cell lines (Fig. 5A). Six serial two-fold dilutions were examined at the following starting doses for BHP7–13, K1, FTC-133 and RO82-W-1, respectively: volasertib at 72.4 nmol/L, 239.2 nmol/L, 86.4 nmol/L and 286.0 nmol/L and sorafenib at 2.8 mmol/L, 18.0 mmol/L, 23.6 mmol/L and 31.2 mmol/L. The starting doses of volasertib and sorafenib were 4-fold IC_{50} of each drug for each cell line determined in this and previous studies (Figure 1, Supplementary Fig. 4, Lin *et al.* 2018). In BHP7–13, K1 and FTC-133 cells, the combination of volasertib and sorafenib had significantly improved cytotoxicity over single agent therapies across all doses of treatment. In RO82-W-1 cells, volasertib and sorafenib combination therapy significantly improved cytotoxicity over single agent therapies at lower doses of treatment. The CI of volasertib and sorafenib was analyzed using the Chou-Talalay method, which revealed that the combination of volasertib and sorafenib ranged from synergistic to antagonist in BHP7–13 cells (CI; 0.83–1.80), K1 cells (CI; 0.65–1.08), and RO82-W-1 cells (CI; 0.60–1.31), and synergistic in FTC-133 cells (CI; 0.41–0.62; Fig. 5B). These data demonstrated that combination therapy of volasertib and sorafenib were mostly synergistic in BHP7–13, K1, FTC-133 and RO82-W-1 cell lines.

Combination therapy of volasertib and sorafenib for murine flank thyroid tumors

We sought to evaluate the effect of volasertib and sorafenib combination therapy in mice bearing K1 and FTC-133 xenografts. Animals with established K1 flank tumors with a mean diameter of 4.3 mm were treated with oral gavage of placebo, volasertib, sorafenib or combination therapy ($n = 6$ per group) once a day for three cycles of therapy (Fig. 6A). The dose of sorafenib was chosen based on a previous report (Lin *et al.* 2018). Volasertib, sorafenib and combination treatment significantly inhibited K1 tumor growth as compared with control treatment (Fig. 6A). The difference in inhibitory effect between volasertib alone and combination therapy did not achieve statistical significance ($P = 0.911$). Serial treatment of volasertib, sorafenib and combination therapy did not significantly result in decrease in body weight as compared with control treatment (Fig. 6B).

Animals with established FTC-133 flank tumors with a mean diameter of 5.5 mm were treated with oral gavage of placebo ($n = 6$), volasertib ($n = 6$), sorafenib ($n = 5$) or combination therapy ($n = 5$) once a day for three cycles of therapy (Fig. 6C). Single volasertib and sorafenib did not significantly retarded FTC-133 tumor growth as compared

with control treatment. However, combination of volasertib and sorafenib treatment significantly inhibited FTC-133 tumor growth as compared with volasertib, sorafenib and placebo therapy. Of noted, combination therapy led to tumor volume reduction in 2 out of 5 animals between days 14 and 35, demonstrating the combination of these two drugs was able to reduce the tumor mass in 40% of FTC-133 xenografts. Serial treatment of volasertib, sorafenib or combination therapy did not result in substantial changes in body weight as compared with control treatment (Fig. 6D). Representative mice bearing FTC-133 tumors were photographed after 21 and 41-day treatment (Fig. 6E). PCNA levels decreased and cleaved caspase-3 levels increased with volasertib treatment in FTC-133 xenografts (Supplementary Fig. 5). Volasertib treatment has demonstrated to increase PLK1 expression in HeLa cells (Raab *et al.* 2015). We observed similar effects of volasertib to increase PLK1 levels in WDTC *in vitro* (Supplementary Fig. 6A) and *in vivo* (Supplementary Fig. 6B).

Discussion

Volasertib effectively inhibited cell survival in papillary and follicular thyroid cancer cell lines. Volasertib treatment alone and in combination with sorafenib effectively inhibited tumor growth of well-differentiated thyroid cancer xenograft models with promising safety profiles. These favorable results suggest that volasertib has the potential for clinical application in the treatment of patients with WDTC.

Volasertib inhibited mitotic progression at prometaphase, which is likely one of the mechanisms of cytotoxicity in the treatment of thyroid cancer cells. Besides mitotic arrest, we also noted that volasertib accumulated cells in G2 phase for BHP7–13, K1, FTC-133 and RO82-W-1 cell lines. Volasertib increased the proportion of G2/M phase cells over that of M phase cells, indicating that volasertib arrests cells in G2 phase. Therefore, G2 phase block is likely a key mechanism of cytotoxicity in the treatment of thyroid cancer cells with volasertib. The inhibition of PLK1 may account for G2 arrest and mitotic block. The main PLK1 functions start in G2 and are essential for mitotic entry and mitotic progression (Zitouni *et al.* 2014, Strebhardt & Ullrich 2006). The effects of PLK1 inhibition may range from a failure of G2/M transition to mitotic arrest. In this study, volasertib consistently inhibited G2/M transition and induced mitotic block in the second mitotic phase (prometaphase) in four cell lines. We found GSK461364, a selective PLK1 inhibitor, also leaded to G2 arrest and mitotic block in WDTC cell lines (Supplementary Fig. 7). Inactivation of PLK3 has demonstrated to induce G2/M arrest (Wang *et al.* 2002).

Volasertib decreased cells in S phase in BHP7–13, K1, FTC-133 and RO82-W-1 cells, which is likely another therapeutic mechanism of volasertib in WDTC cell lines. A failure of entry from G1 to S phase may account for the decreased cells in S phase. PLK2 and PLK3 are pivotal for the process of G1/S transition. PLK2 is required for centriole duplication and onset of S phase (Cizmecioglu *et al.* 2012). Depletion of PLK2 leads to delay entry into S phase (Ma *et al.* 2003). PLK3 expression is peak in G1 phase, and inhibition of PLK3 results in prevention of S phase entry (Zimmerman & Erikson 2007). The ability of volasertib to inhibit PLK2 and PLK3 may contribute to the failure of G1/S transition and subsequently decrease cells in S phase in thyroid cancer cells. Another explanation for the decreased cells at S phase may be as a result of fewer cell entering G1 phase because of G2/M arrest.

Tumor cells often escape apoptosis and induction of apoptosis is considered an important mechanism of anti-cancer therapies. PLK1 is involved in the regulation of apoptosis; therefore, inhibition of PLK1 activity is likely to contribute to the apoptotic response (Liu & Erikson 2003). Volasertib treatment activated caspase-3 activity and induced apoptosis in WDTC cell lines, which is likely one of the mechanisms of cytotoxicity in the treatment of thyroid cancer.

RO82-W-1 cells were the least sensitive cell line to volasertib treatment in terms of the highest IC_{50} among 4 WDTC cell lines. RO82-W-1 cells were more resistant to sub-G1 apoptosis induced by volasertib treatment. In addition, RO82-W-1 cells had a relatively slower cell proliferation rate (Supplementary Fig. 8). Slow growing cells are likely less sensitive to cell cycle inhibition as compared with rapid growing cells. These observations may account for the less sensitivity of RO82-W-1 cells to volasertib therapy.

Volasertib treatment significantly repressed K1 tumor growth. The anti-tumor effects are likely mediated through both cell cycle inhibition and apoptosis induction given that PCNA levels decreased and cleaved caspase-3 levels increased with volasertib treatment in K1 xenografts.

Sorafenib therapy is an U.S. FDA-approved treatment for WDTC. However, many patients with refractory WDTC stop sorafenib treatment because of side effects or treatment failures. Devising novel strategies to augment the therapeutic effects of sorafenib is essential. In this study, we found promising therapeutic effects of volasertib and sorafenib combination therapy in the treatment of FTC-133 tumors. This combination therapy inhibited FTC-133 tumor growth significantly as compared with either drug treatment alone with favorable safety profiles.

To explore potential biomarkers that correlate with sensitivity of volasertib, the baseline expression of PLK1, PLK2 and PLK3 were evaluated in four WDTC cell lines (Supplementary Fig. 9A). The sensitivity of these cell lines to volasertib was ordered according to the IC_{50} value. Statistical relationships were analyzed using Pearson's correlation coefficient (Supplementary Fig. 9B). The expression of PLK1, PLK2 and PLK3 failed to show any significant correlation with volasertib sensitivity in WDTC cells.

We found volasertib treatment led to increased PLK1 expression in WDTC *in vitro* and *in vivo*. The reasons accounting for this phenomenon are unclear. One tentative explanation is PLK1 expression was increased to compensate the decreased activity of PLK1.

A recent report reveals the combination of volasertib and PI3K inhibitors was synergistic in the treatment of anaplastic thyroid cancer (ATC) cells *in vitro* (De Martino *et al.* 2018). Combining volasertib and a PI3K inhibitor was more effective in inhibiting ATC tumor growth than either single agent therapy and placebo treatment. These findings are encouraging and potentially broaden the clinical applications of volasertib in the treatment of thyroid cancer. Besides, many PLK inhibitors are under clinical evaluation in the treatment of cancers (ClinicalTrials.gov, accessed April 11, 2019).

RO82-W-1 and WRO82–1 are considered to be the same cell line with different designations (SIB Bioinformatics Resource Portal, accessed May 24, 2019). However, we found the DNA STR profiling of RO82-W-1 cells was different to that of WRO82–1 cells (Supplementary Figures 10, Schweppe *et al.* 2008). We acknowledge RO82-W-1 is not the same as WRO82–1. Besides, our data reveals RO82-W-1 cells had wild-type *BRAF* V600.

Conclusions

Volasertib induces cytotoxicity in both papillary and follicular thyroid cancer cell lines. The therapeutic efficacy and safety of volasertib treatment were demonstrated in a xenograft mouse model. Volasertib and sorafenib combination therapy exhibited greater therapeutic efficacy over either single treatment in FTC-133 tumors. These data support the clinical evaluation of volasertib in the treatment of patients with WDTC.

Supplementary Material

Refer to Web version on PubMed Central for supplementary material.

Acknowledgements

We thank the staff of the Microscope Core Laboratory, the Laboratory Animal Center, and the Expensive Advanced Instrument Core Laboratory of the Chang Gung Memorial Hospital at Linkou for technical support.

Funding

This work was supported by the Chang Gung Memorial Hospital (CMRPG3H0201, CMRPG3E0353) and the Ministry of Science and Technology of Taiwan (MOST 106-2314-B-182A-095-).

References

Brose MS, Nutting CM, Jarzab B, Elisei R, Siena S, Bastholt L, de la Fouchardiere C, Pacini F, Paschke R, Shong YK, et al. 2014 Sorafenib in radioactive iodine-refractory, locally advanced or metastatic differentiated thyroid cancer: a randomised, double-blind, phase 3 trial. Lancet 384 319–328. [PubMed: 24768112]

Cabanillas ME, McFadden DG & Durante C 2016 Thyroid cancer. Lancet 388 2783–2795. [PubMed: 27240885]

Chou TC 2006 Theoretical basis, experimental design, and computerized simulation of synergism and antagonism in drug combination studies. Pharmacology Review 58 621–681.

Chou TC & Martin N 2005 CompuSyn for drug combinations: PC software and users guide: a computer program for quantitation of synergism and antagonism in drug combinations and the determination of IC50, ED50, and LD50 values. Paramus, NJ, USA: ComboSyn.

Cizmecioglu O, Krause A, Bahtz R, Ehret L, Malek N & Hoffmann I 2012 Plk2 regulates centriole duplication through phosphorylation-mediated degradation of Fbxw7 (human Cdc4). Journal of Cell Science 125 981–992. [PubMed: 22399798]

de Cárcer G, Manning G & Malumbres M 2011a From Plk1 to Plk5: functional evolution of polo-like kinases. Cell Cycle 10 2255–2262. [PubMed: 21654194]

de Cárcer G, Escobar B, Higuero AM, García L, Ansón A, Pérez G, Mollejo M, Manning G, Meléndez B, Abad-Rodríguez J, et al. 2011b Plk5, a polo box domain-only protein with specific roles in neuron differentiation and glioblastoma suppression. Molecular and Cellular Biology 31 1225–1239. [PubMed: 21245385]

De Martino D, Yilmaz E, Orlacchio A, Ranieri M, Zhao K & Di Cristofano A 2018 PI3K blockage synergizes with PLK1 inhibition preventing endoreduplication and enhancing apoptosis in anaplastic thyroid cancer. Cancer Lett 439 56–65. [PubMed: 30243708]

Durante C, Haddy N, Baudin E, Leboulleux S, Hartl D, Travagli JP, Caillou B, Ricard M, Lumbroso JD, De Vathaire F, et al. 2006 Long-term outcome of 444 patients with distant metastases from papillary and follicular thyroid carcinoma: benefits and limits of radioiodine therapy. J Clin Endocrinol Metab 91 2892–2899. [PubMed: 16684830]

Fagin JA & Wells SA Jr 2016 Biologic and Clinical Perspectives on Thyroid Cancer. New England Journal of Medicine 375 1054–1067. [PubMed: 27626519]

Gjertsen BT & Schöffski P 2015 Discovery and development of the Polo-like kinase inhibitor volasertib in cancer therapy. Leukemia 29 11–19. [PubMed: 25027517]

Habedanck R, Stierhof YD, Wilkinson CJ & Nigg EA 2005 The Polo kinase Plk4 functions in centriole duplication. Nature Cell Biology 7 1140–1146. [PubMed: 16244668]

Helmke C, Becker S & Strebhardt K 2016 The role of Plk3 in oncogenesis. Oncogene 35 135–147. [PubMed: 25915845]

Kitahara CM & Sosa JA 2016 The changing incidence of thyroid cancer. Nature Reviews Endocrinology 12 646–653.

Kosco K, Ridinger M, Whitley P, Croucher P, Miner JN & Erlander M 2018 Selective Polo-like Kinase 1 (PLK1) inhibitor PCM-075 is highly active alone and shows synergy when combined with FLT3 inhibitors in models of acute myeloid leukemia (AML). Cancer Res 78(13 Suppl) Abstract nr 1885.

Lin SF, Lin JD, Hsueh C, Chou TC & Wong RJ 2017 A cyclin-dependent kinase inhibitor, dinaciclib in preclinical treatment models of thyroid cancer. PLOS ONE 12 e0172315. [PubMed: 28207834]

Lin SF, Lin JD, Hsueh C, Chou TC & Wong RJ 2018 Potent effects of roniciclib alone and with sorafenib against well-differentiated thyroid cancer. Endocrine-Related Cancer 25 853–864. [PubMed: 29895526]

Liu X & Erikson RL 2003 Polo-like kinase (Plk)1 depletion induces apoptosis in cancer cells. Proceedings of the National Academy of Sciences 100 5789–5794.

Ma S, Charron J & Erikson RL 2003 Role of Plk2 (Snk) in mouse development and cell proliferation. Molecular and Cellular Biology 23 6936–6943. [PubMed: 12972611]

Moldovan GL, Pfander B & Jentsch S 2007 PCNA, the maestro of the replication fork. Cell 129 665–679. [PubMed: 17512402]

Nguyen T, Parker R, Hawkins E, Holkova B, Yazbeck V, Kolluri A, Kmieciak M, Rahmani M & Grant S 2017 Synergistic interactions between PLK1 and HDAC inhibitors in non-Hodgkin's lymphoma cells occur in vitro and in vivo and proceed through multiple mechanisms. Oncotarget 8 31478–31493. [PubMed: 28416758]

Pfeffer CM & Singh ATK 2018 Apoptosis: A Target for Anticancer Therapy. International Journal of Molecular Sciences 19 448.

Pujade-Lauraine E, Selle F, Weber B, Ray-Coquard IL, Vergote I, Sufliarsky J, Del Campo JM, Lortholary A, Lesoin A, Follana P, et al. 2016 Volasertib Versus Chemotherapy in Platinum-Resistant or -Refractory Ovarian Cancer: A Randomized Phase II Groupe des Investigateurs Nationaux pour l'Etude des Cancers de l'Ovaire Study. Journal of Clinical Oncology 34 706–713. [PubMed: 26755507]

Raab M, Krämer A, Hehlgans S, Sanhaji M, Kurunci-Csacsko E, Dötsch C, Bug G, Ottmann O, Becker S, Pachl F, et al. 2015 Mitotic arrest and slippage induced by pharmacological inhibition of Polo-like kinase 1. Molecular Oncology 9 140–154. [PubMed: 25169932]

Rudolph D, Steegmaier M, Hoffmann M, Grauert M, Baum A, Quant J, Haslinger C, Garin-Chesa P & Adolf GR 2009 BI 6727, a Polo-like kinase inhibitor with improved pharmacokinetic profile and broad antitumor activity. Clinical Cancer Research 15 3094–3102. [PubMed: 19383823]

Rudolph D, Impagnatiello MA, Blaukopf C, Sommer C, Gerlich DW, Roth M, Tontsch-Grunt U, Wernitznig A, Savarese F, Hofmann MH, et al. 2015 Efficacy and mechanism of action of volasertib, a potent and selective inhibitor of Polo-like kinases, in preclinical models of acute myeloid leukemia. Journal of Pharmacology and Experimental Therapeutics 352 579–589. [PubMed: 25576074]

Schlumberger M, Tahara M, Wirth LJ, Robinson B, Brose MS, Elisei R, Habra MA, Newbold K, Shah MH, Hoff AO, et al. 2015 Lenvatinib versus placebo in radioiodine-refractory thyroid cancer. New England Journal of Medicine 372 621–630. [PubMed: 25671254]

Schweppe RE, Klopper JP, Korch C, Pugazhenthi U, Benezra M, Knauf JA, Fagin JA, Marlow LA, Copland JA, Smallridge RC, et al. 2008 Deoxyribonucleic acid profiling analysis of 40 human thyroid cancer cell lines reveals cross-contamination resulting in cell line redundancy and misidentification. Journal of Clinical Endocrinology and Metabolism 93 4331–4341. [PubMed: 18713817]

Sebastian M, Reck M, Waller CF, Kortsik C, Frickhofen N, Schuler M, Fritsch H, Gaschler-Markefski B, Hanft G, Munzert G, et al. 2010 The efficacy and safety of BI 2536, a novel Plk-1 inhibitor, in patients with stage IIIB/IV non-small cell lung cancer who had relapsed after, or failed, chemotherapy: results from an open-label, randomized phase II clinical trial. J Thorac Oncol 5 1060–1067. [PubMed: 20526206]

Shao C, Chien SJ, Farah E, Li Z, Ahmad N & Liu X 2018 Plk1 phosphorylation of Numb leads to impaired DNA damage response. Oncogene 37 810–820. [PubMed: 29059161]

Strebhardt K & Ullrich A 2006 Targeting polo-like kinase 1 for cancer therapy. Nature Reviews Cancer 6 321–330. [PubMed: 16557283]

Strebhardt K 2010 Multifaceted polo-like kinases: drug targets and antitargets for cancer therapy. Nature Reviews Drug Discovery 9 643–660. [PubMed: 20671765]

Wang Q, Xie S, Chen J, Fukasawa K, Naik U, Traganos F, Darzynkiewicz Z, Jhanwar-Uniyal M & Dai W 2002 Cell cycle arrest and apoptosis induced by human Polo-like kinase 3 is mediated through perturbation of microtubule integrity. Molecular and Cellular Biology 22 3450–3459. [PubMed: 11971976]

Yata K, Lloyd J, Maslen S, Bleuyard JY, Skehel M, Smerdon SJ & Esashi F 2012 Plk1 and CK2 act in concert to regulate Rad51 during DNA double strand break repair. Molecular Cell 45 371–383. [PubMed: 22325354]

Zimmerman WC & Erikson RL 2007 Polo-like kinase 3 is required for entry into S phase. Proceedings of the National Academy of Sciences 104 1847–1852.

Zitouni S, Nabais C, Jana SC, Guerrero A & Bettencourt-Dias M 2014 Polo-like kinases: structural variations lead to multiple functions. Nature Reviews Molecular Cell Biology 15 433–452. [PubMed: 24954208]

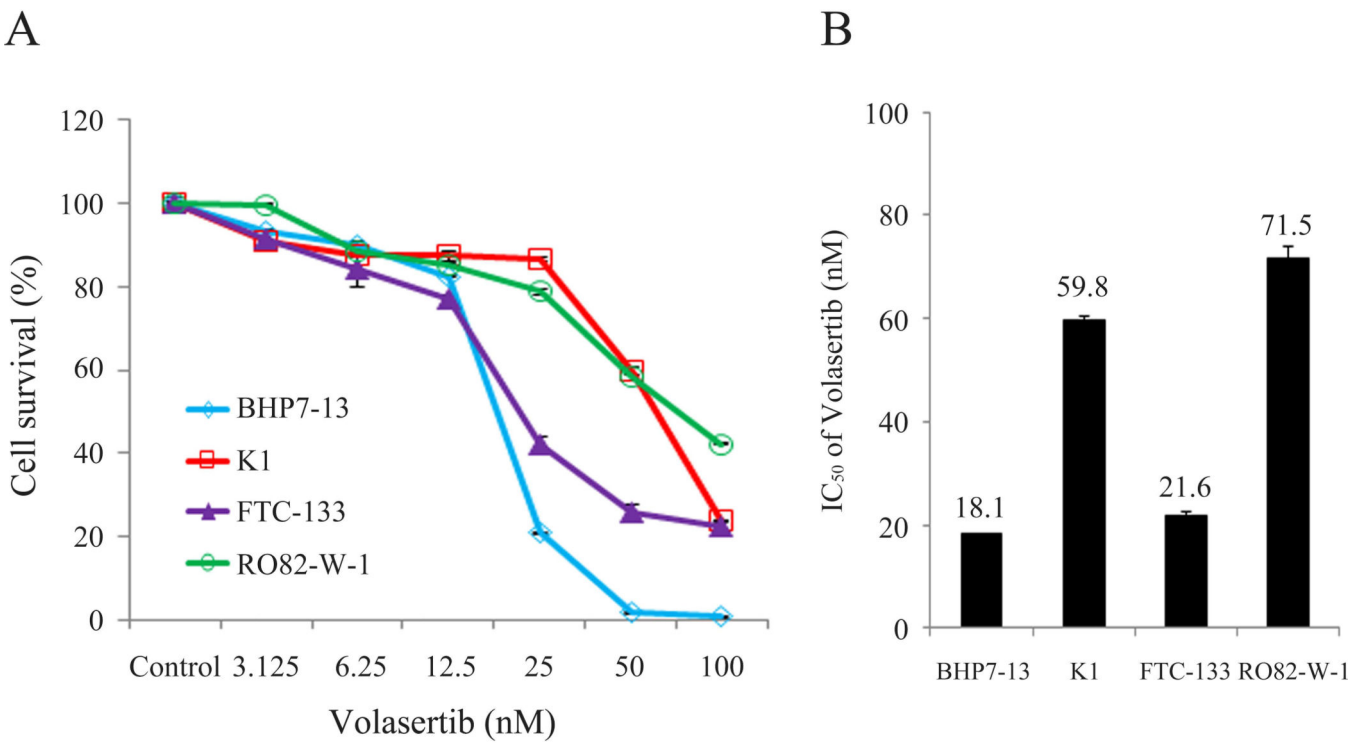

Figure 1. Volasertib induces cytotoxicity in well-differentiated thyroid cancer cells.

(A) Cytotoxicity was evaluated in cells treated with a series of six two-fold dilutions of volasertib starting from 100 nmol/L. Dose-response curves were obtained on day 4 using LDH assays. (B) The median-effect dose (IC_{50}) of volasertib on day 4 was calculated for each cell line using CompuSyn software.

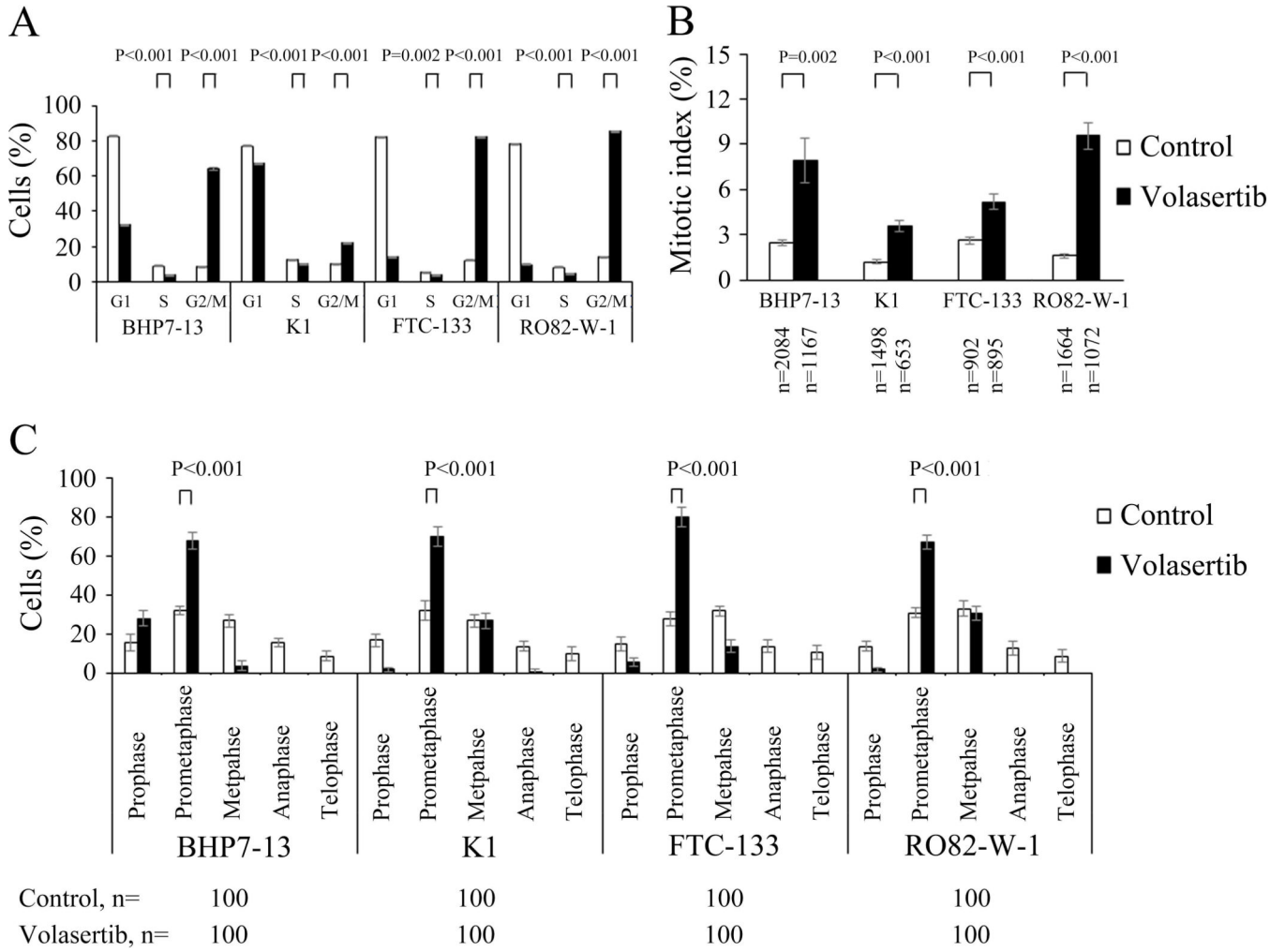

Figure 2. Volasertib decreases cells in S phase, accumulates cells in G2/M phase and inhibits mitotic progression in prometaphase in well-differentiated thyroid cancer cells.

(A) Cell cycle distribution was analyzed by evaluating the DNA content in well-differentiated thyroid cancer cells treated with placebo or volasertib (100 nmol/L) for 24 h using flow cytometry. Volasertib treatment significantly reduced cells in S phase and accumulated cells in G2/M phase in four cell lines. (B) The proportion of well-differentiated thyroid cancer cells in mitosis was assessed after treatment with volasertib (100 nmol/L) or placebo for 24 h. Cells were stained with DAPI, and chromosome characteristics were evaluated using immunofluorescence confocal microscopy. The mitotic index was assessed with a minimum of 653 cells counted from 10 different fields for each condition. Volasertib significantly increased the proportion of BHP7–13, K1, FTC-133 and RO82-W-1 cells in mitosis. (C) The distribution of cells in mitosis was determined by counting 100 mitotic cells by confocal microscopy for each condition. Quantification analyses revealed mitotic cells were arrested in prometaphase by the treatment of volasertib (100 nmol/L) for 24 h.

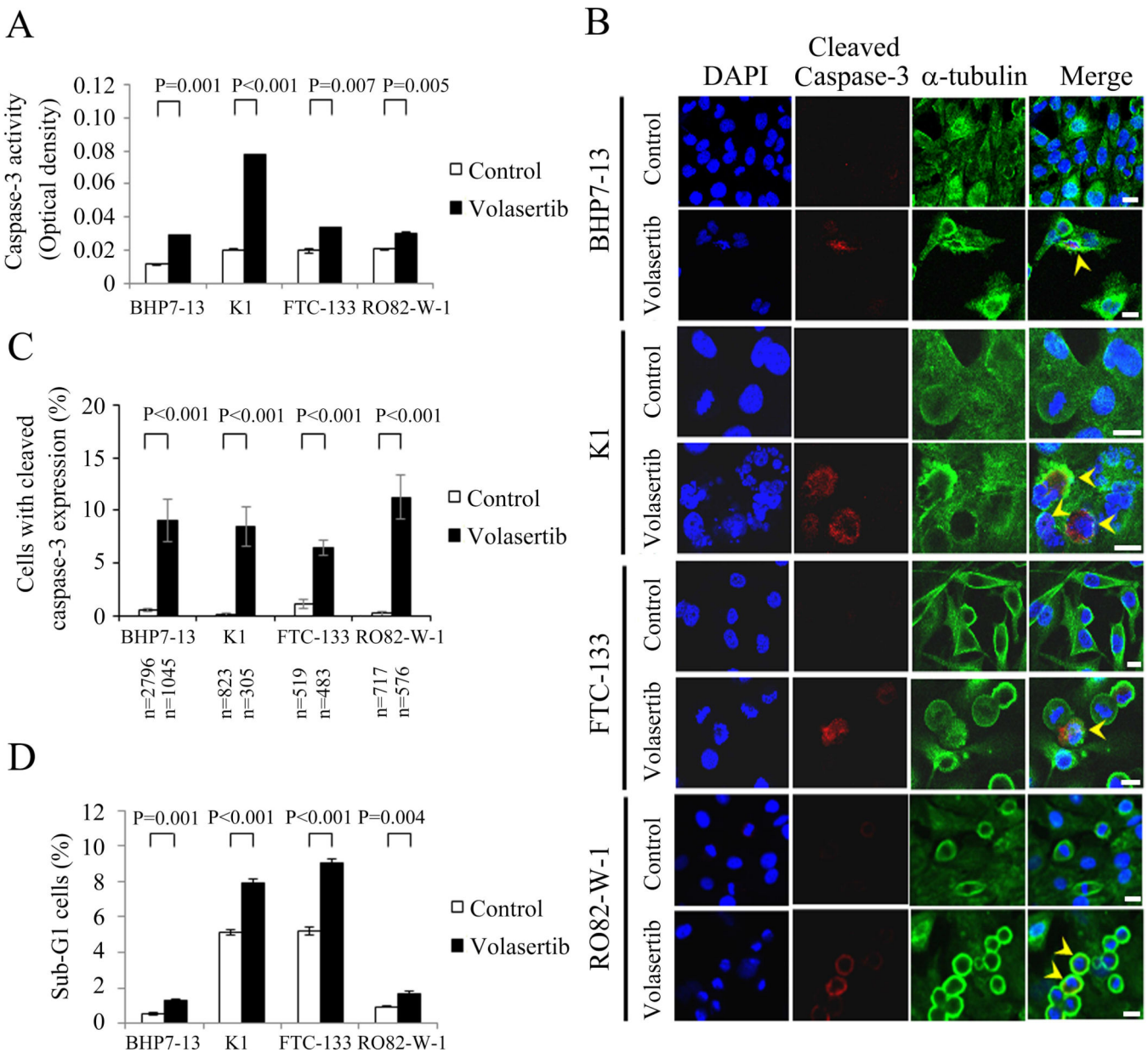

Figure 3. Volasertib stimulates caspase-3 activity and induces apoptosis in well-differentiated thyroid cancer cells.

(A) Caspase-3 activity was evaluated using a fluorometric assay kit in BHP7–13, K1, FTC-133 and RO82-W-1 cells treated with Volasertib (100 nmol/L) or vehicle for 24 h. (B) Well-differentiated thyroid cancer cells were treated with volasertib (100 nmol/L) or placebo for 24 h and stained with DAPI (blue) and fluorescent antibodies against cleaved caspase-3 (red) and α-tubulin (green). Cells with cleaved caspase-3 expression are shown (arrowhead). (C) The percentages of cells with cleaved caspase-3 expression were assessed after treatment with placebo or volasertib (100 nmol/L) for 24 h. Cells were stained with fluorescent antibodies against cleaved caspase-3, and its expression was evaluated using immunofluorescence confocal microscopy. A minimum of 305 cells from at least 10 different fields was counted for each condition. Volasertib significantly increased the

proportion of BHP7–13, K1, FTC-133 and RO82-W-1 cells with cleaved caspase-3 expression. (D) Sub-G1 apoptotic cells were detected by measuring the DNA content of 1×10^4 events for each sample using flow cytometry in cells treated with volasertib (100 nmol/L) or vehicle for 24 h. Volasertib increased the proportion of sub-G1 cells in four well-differentiated thyroid cancer cell lines. Scale bar, 20 μm.

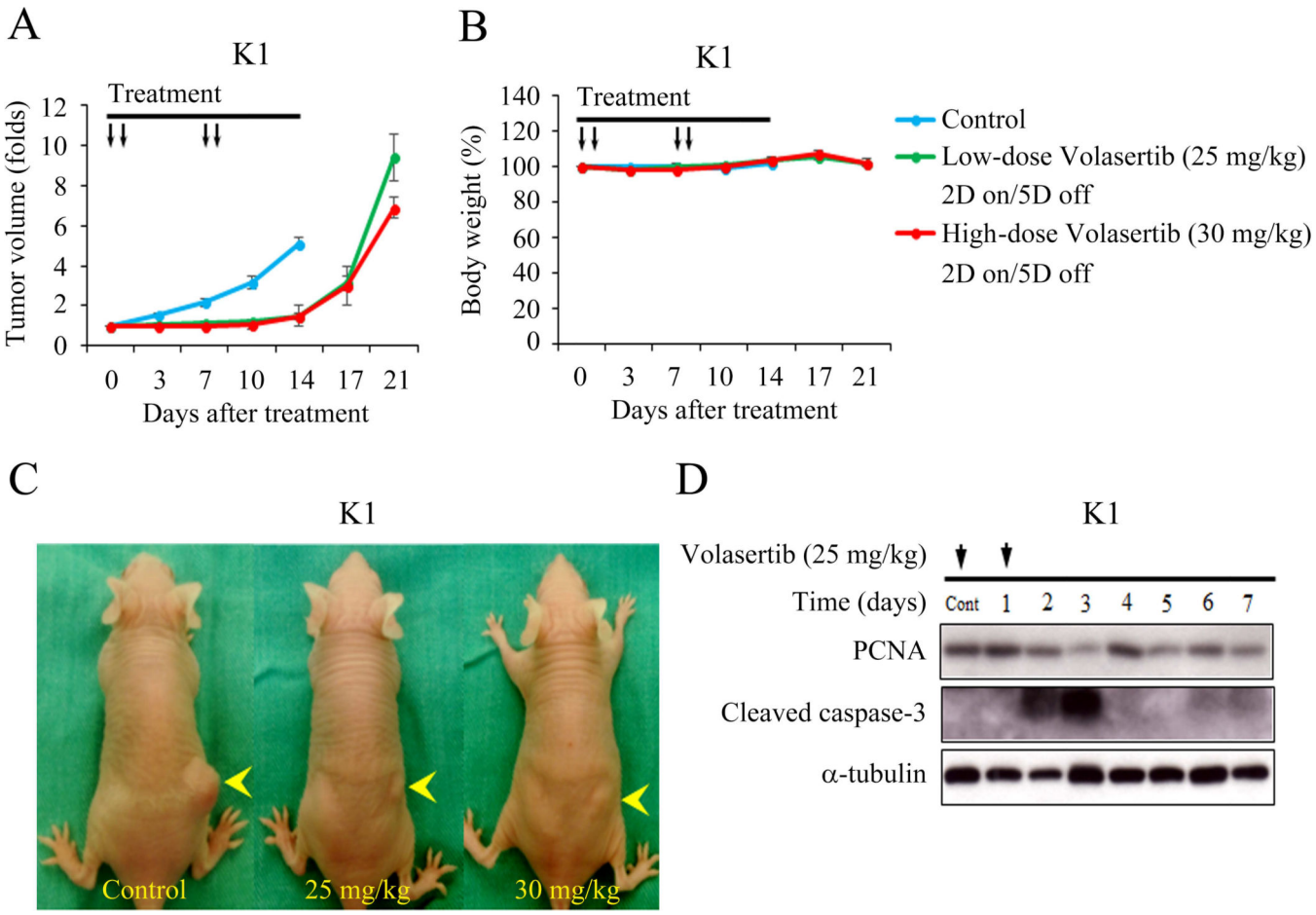

Figure 4. Volasertib inhibits subcutaneous xenograft growth of a well-differentiated thyroid cancer model.

(A) The therapeutic efficacy of volasertib for papillary thyroid cancer was evaluated in mice bearing K1 flank tumors. Serial oral gavage of low-dose (25 mg/kg) and high-dose (30 mg/kg) volasertib significantly repressed K1 tumor growth as compared with control treatment. (B) Serial treatment of low-dose and high-dose volasertib did not significantly decrease body weight as compared with control mice. (C) K1 xenograft tumors (arrowhead) were photographed on day 14. (D) The molecular effects of volasertib (25 mg/kg) treatment were evaluated in K1 tumors using Western blot analysis. Arrow, volasertib or placebo treatment.

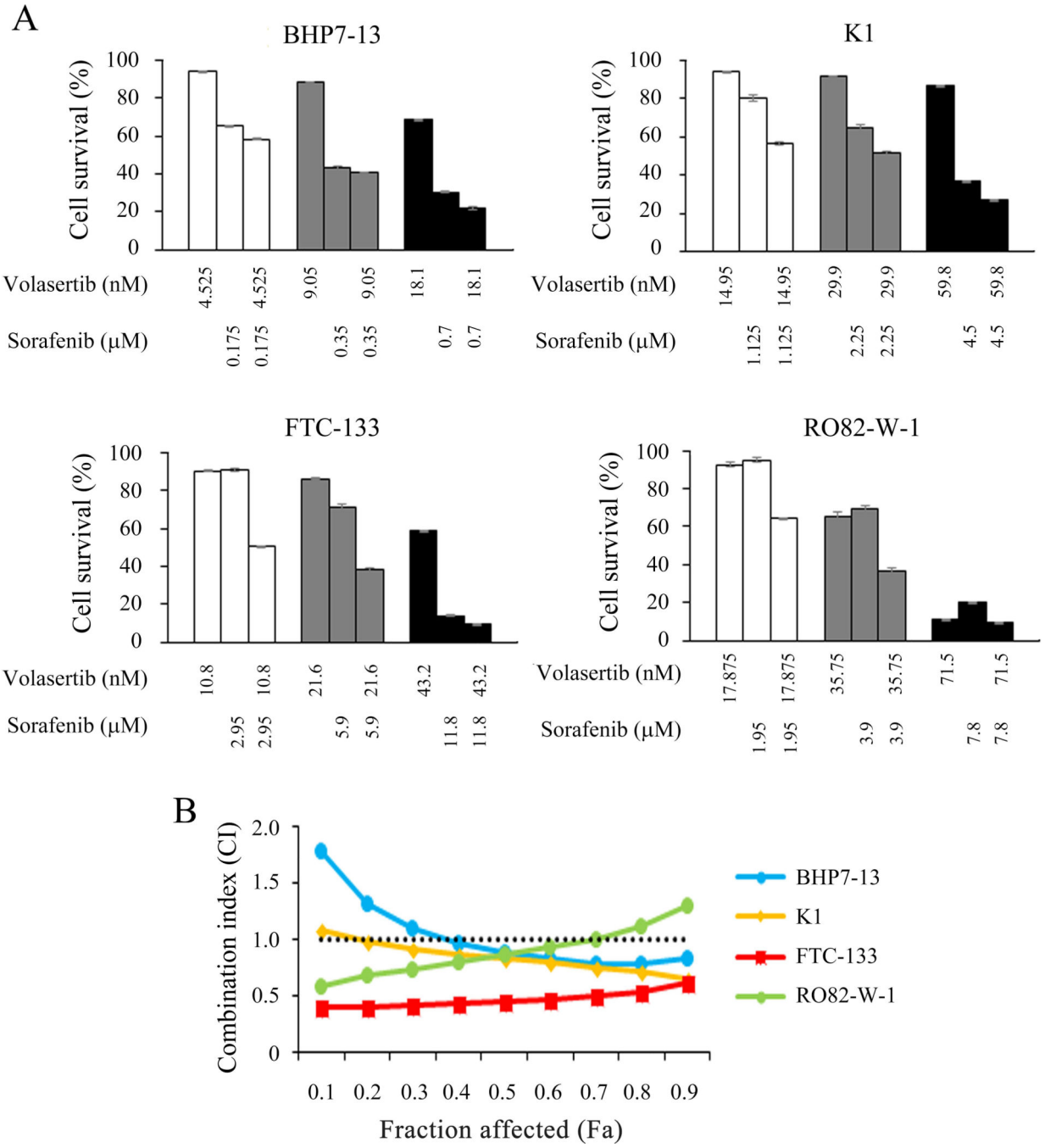

Figure 5. Combination therapy of volasertib and sorafenib in well-differentiated thyroid cancer cells.

(A) The cytotoxic effects of volasertib and sorafenib alone and in combination after a 4-day treatment in BHP7–13, K1, FTC-133 and RO82-W-1 cells were evaluated using LDH assays. (B) The combination index (CI) of volasertib and sorafenib was calculated using CompuSyn software. The combination therapy of volasertib and sorafenib had synergistic effects in FTC-133 cells, and synergistic to antagonistic effects in BHP7–13, K1 and RO82-W-1 cells. Volasertib plus sorafenib appeared synergistic effects at most conditions in BHP7–13, K1 and RO82-W-1 cell lines. The horizontal line at CI = 1 was drawn for

discrimination of synergism (CI < 1) and antagonism (CI > 1). Fraction affected (Fa) means the proportion of cell inhibition (percent inhibition/100).

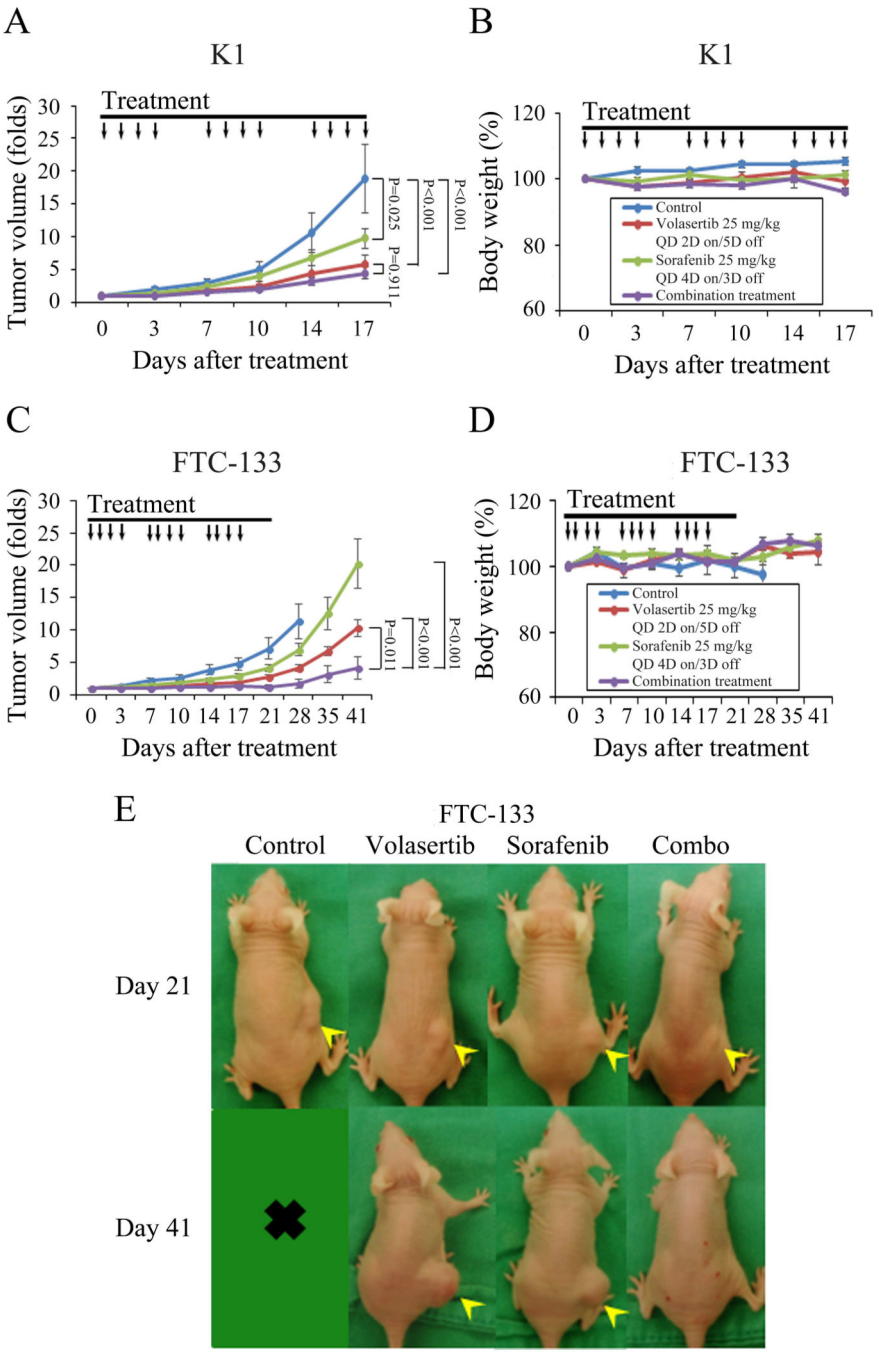

Figure 6. Therapeutic effects of volasertib and sorafenib in murine K1 and FTC-133 xenograft tumor models.

(A) After K1 flank tumors were established in nude mice, mice were treated with oral gavage of placebo, volasertib (25 mg/kg, 2-day on and 5-day off), sorafenib (25 mg/kg, 4-day on and 3-day off) or combination therapy once a day for three cycles of therapy. Compared with control therapy, volasertib, sorafenib and combination treatment significantly inhibited tumor growth. Combination therapy did not significantly retarded xenograft growth when compared with volasertib or sorafenib single modality treatment. (B) Volasertib, sorafenib and combination therapy did not significantly decrease body weight as

compared with control mice. (C) After FTC-133 flank tumors were established in nude mice, they were treated with oral gavage of placebo, volasertib (25 mg/kg, 2-day on and 5-day off), sorafenib (25 mg/kg, 4-day on and 3-day off) or combination therapy for three cycles of therapy. Compared with control therapy, volasertib and sorafenib treatment did not significantly inhibited tumor growth. However, combination therapy significantly retarded xenograft growth when compared with either single agent and control treatment. (D) No substantial decreases in body weight were attributable to volasertib, sorafenib or combination therapy compared with the control mice. (E) Mice bearing FTC-133 tumors (arrowhead) were photographed on days 21 and 41. Arrow, placebo, volasertib, sorafenib and combination treatment.